Power Conditioner for AC PV Systems Using GA

Luis David Pabon Fernandez(✉), Edison Andres Caicedo Peñaranda(✉), and Jorge Luis Diaz Rodriguez(✉)

Universidad de Pamplona, Pamplona, Colombia

Abstract. This work presents the development of a multilevel power inverter prototype with the use of optimized modulation which manages to significantly minimize the harmonic content of output voltages using Genetics Algorithms. Additionally, it integrates a DC/DC converter that allows to regulate the RMS value of the inverter output voltage through the control of the DC bus voltage. A control loop is implemented that allows obtaining the optimal power quality by verifying compliance with the IEEE 1159 (1995) and IEEE 519 (1992) standards. Through this it is possible to avoid most of the related power quality phenomena such as sag, swell, flicker, undervoltage, etc. Finally, the prototype was successfully implemented and verified.

Keywords: Multilevel converter · PWM · Optimization · Genetic algorithm · THD

1 Introduction

Photovoltaic (PV) systems are used to power loads in alternating current (AC) system, thus the need of electrical power inverters is essential, since solar panels generate electric power of direct current (DC) [1, 2]. The conversion of the electrical power usually uses control strategies involving power inverters with PWM modulation [3], for this purpose. Commonly, these techniques involve switching and harmonic distortion problems [4, 5]. To solve these problems and achieve a voltage waveform closer to a pure sinewave waveform, with the minimum of power switching devices. The alternative of using a new family of inverters arises: the multilevel power converters [6–8].

The idea of using multiple voltage levels to carry out electrical conversion was proposed in 1975, nevertheless the multilevel power converter was first implemented with the three-step inverter introduced by Nabae, Takahashi, and Akagi in 1981 [9]. Subsequently, several topologies of multilevel converters have been developed, which have in common the elementary concept of achieving stepped voltage waves that are closer to a sinusoidal waveform [10, 11].

To bring the waveforms of the voltages of multilevel converters even closer to pure sinusoidal waveforms, multiple harmonic content optimization works have been carried out [12–14]. These works pursue the elimination of harmonics, either in selective orders [15, 16] or in a certain range or determined band [17]. However, a definitive optimum is not achieved (the subject is currently under research).

J. C. Figueroa-García et al. (Eds.): WEA 2021, CCIS 1431, pp. 133–144, 2021.
https://doi.org/10.1007/978-3-030-86702-7_12

Another problem of the DC/AC conversion in PV systems is the variation of the voltage in terms of the load changes and fluctuations of the accumulator block or of the solar panels from which the inverter takes the energy [15]. In power inverters, voltage regulation can cause the output voltages to go further the limits to preserve the power quality to the load.

This work presents a prototype of a multilevel inverter that uses evolutionary techniques to optimize the harmonic content of the output voltages. As it integrates as a previous stage a DC/DC converter, that regulate the RMS value of the inverter output voltage, by means of controlling the DC bus voltage. In this way, the power quality of PV systems has been optimized, thus avoiding phenomena such as sag, swell, flicker, undervoltage, overvoltage, interharmonics, frequency deviations and DC shifts and with a minimum of total harmonic distortion (THD).

2 Two-Stage Multilevel Converter Per Phase

To mitigate the power quality phenomena associated with the RMS value, voltage control is performed on the DC bus side through a DC/DC converter. The selected converter to carry out this task is the non-inverting step-down converter of reduced elements [17]. The schematic of the CD/CD converter is shown in Fig. 1a.

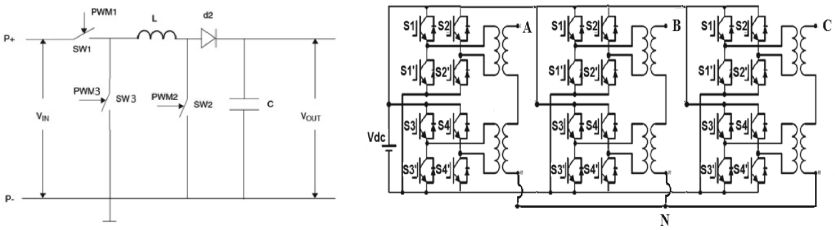

Fig. 1. Circuit a) of the DC/DC converter b) Topology of the multilevel inverter

A modification to the original topology was included, by changing a blocking diode for the switching element called SW3 in Fig. 1. This in order to carry out a simpler activation process for switch SW1, using a circuit simple bootstrap circuit.

To mitigate the phenomena associated with the waveform and to generate voltages with harmonic optimization, the multilevel inverter topology selected for this work is the common source asymmetric H-bridge cascaded converter with a 1:3 ratio and 2 power stages. The power converter generates a line voltage with a maximum of 17 steps, this topology is shown in Fig. 1b [16].

These two converters are connected in cascaded in order to obtain the electrical power inverting and conditioning prototype for PV systems that require an AC output.

3 Mathematical Modeling

3.1 Line Voltaje THD

The IEEE 519 (1992) standard defines total harmonic distortion as follows (3) [18].

$$THD = \frac{\sqrt{\sum_{n=2}^{50} h_n^2}}{h_1} \cdot 100 \tag{1}$$

Where the harmonic h_1 is the fundamental component and h_n is the peak of the harmonic n. Using this expression and previous works by the authors [13, 17], this expression becomes:

$$THD = \frac{\sqrt{\sum_{n=2}^{50}\left(\frac{1}{n}\left[\sum_{i=1}^{4}\sum_{j=1}^{Li}(-1)^{j-1}\cos n\alpha_{ij}\right]\right)^2}}{\left[\sum_{i=1}^{4}\sum_{j=1}^{Li}(-1)^{j-1}\cos 1\alpha_{ij}\right]} * 100 \tag{2}$$

Where n takes odd values not multiples of three, that is, 5, 7, 11, 13, 17, etc. and L_i are the components of the vector $L = [a\ b\ c\ d]$. which index how many angles each step has in the first quarter wave of the modulation. Similarly, the effective value can be defined in terms of harmonics as:

$$Vline_{RMS} = \sqrt{\sum_{n=1}^{\alpha} Vrms_n^2} \tag{3}$$

Replacing an upper bound $h_{max} = 50$ the Vrms is determined by Eq. 4:

$$Vline_{RMS} = \sqrt{\sum_{n=1}^{50} \frac{\left(\frac{4\sqrt{3}Vdc}{\pi n}\left[\sum_{i=1}^{4}\sum_{j=1}^{Li}(-1)^{j-1}\cos n\alpha_{ij}\right]\right)^2}{2}} \tag{4}$$

$$for\ n = 5, 7, \ldots odd\ not\ multiples\ of\ three$$

In this way, Eq. (2) defines the THD equation as the objective function to be minimized by the optimization algorithm and Eq. (4) define the second objective equation that will search for the effective value desired by the user. In this way the algorithm will find a modulation with an RMS value. This will be defined as rated by the user and with the harmonic distortion as close to zero percent. In Eqs. (2) and (4) the harmonics evaluated are the odd and non-triple ones.

This is because harmonics multiples of three have been cancel out in line voltages, and can exist in phases. However, as the converter will be applied to a PV system where single-phase loads can be connected, the evaluation of the two functions will consider the harmonics multiples of three in order for the optimization to be carried out in both the phase and line voltages.

4 Optimization Algorithm

To obtain a power inverter that improves the quality of the energy, which should guarantee in ideal conditions that the voltage at the output of the device must be free of harmonic distortions, and at the same time be capable of maintaining the level of the constant voltage and equal to rated voltage.

With the multilevel converter, it is possible to obtain a low distortion voltage waveform with low switching, however, the switching angles must be calculated so that the harmonic distortion is low. This involves solving Eq. (2) with commutation angles by making the THD value as close to zero. However, this can cause the RMS value of the voltage to be far from the desired value. In this way, the solution of Eq. (2) must be restricted so that Eq. (4) results in a value as close as possible to the value of the desired line voltage. A technique must be used to solve this problem that allows approaching a solution that optimizes the THD value and maintains a desired RMS voltage value. The performance of the DC/DC converter is limited to correcting variations due to voltage regulation low voltage levels on the DC bus.

A multiobjective genetic algorithms were used as an optimization technique. In order to make the THD equation as close as possible to zero and the Vrms equation to as close as possible to 220 V. This will be the rated line voltage of the prototype; to achieve these objectives we will used the algorithm shown in Fig. 2.

The main fitness function will be Eq. (2) that allows the THD value to be calculated. This function should be as close as possible to zero percent, the restriction will be taken as Eq. (4) in such a way that the line voltage is as close as possible to a voltage of 220 V.

In the algorithm, the rated values of the machine are assigned first, the line voltage (V_n) and rated frequency (f_n). Then the user gives the maximum number of generations with which the multiobjective genetic algorithm must operate (Nmax), then an initial vector L is assigned to start the RMS and THD value calculations and the respective evolution. The algorithm assigns a vector of the switching angles L = [a b c d]. The vector L contains the information of how many switching angles to be generated in each of the four steps of the first quarter wave of the converter phase voltage. With this information, an initial population P(X) of 20 individuals, where X are the vectors of the created waveform.

The algorithm creates an initial population of 20 individuals that evolves in terms of the performance of the two fitness functions given by the THD and VRMS equations, in each generation of evolution. The algorithm selects the individuals with the lowest THD and whose RMS voltage value is closest to the rated value. At this stage, the use of evolutionary operators is presented, the percentage of the population to perform elitism is only 5%. The *CrossoverFraction* is the fraction of genes swapped between individuals is 0.8. The fraction of population on non-dominated front *ParetoFraction* is 0.35. In each generation these operators are applied and the evolution of the THD value is reviewed and restricted to compliance with the RMS value of the line voltage.

In this way, the algorithm will evolve until it reaches some convergence criteria, which are: if the THD and the RMS values converge or if the THD is null and the RMS value is the desired one or the maximum number of generations is fulfilled, the evolutionary part of the algorithm ends. If these conditions are not met, the algorithm applies the evolutionary operators to the population and begins with another generation.

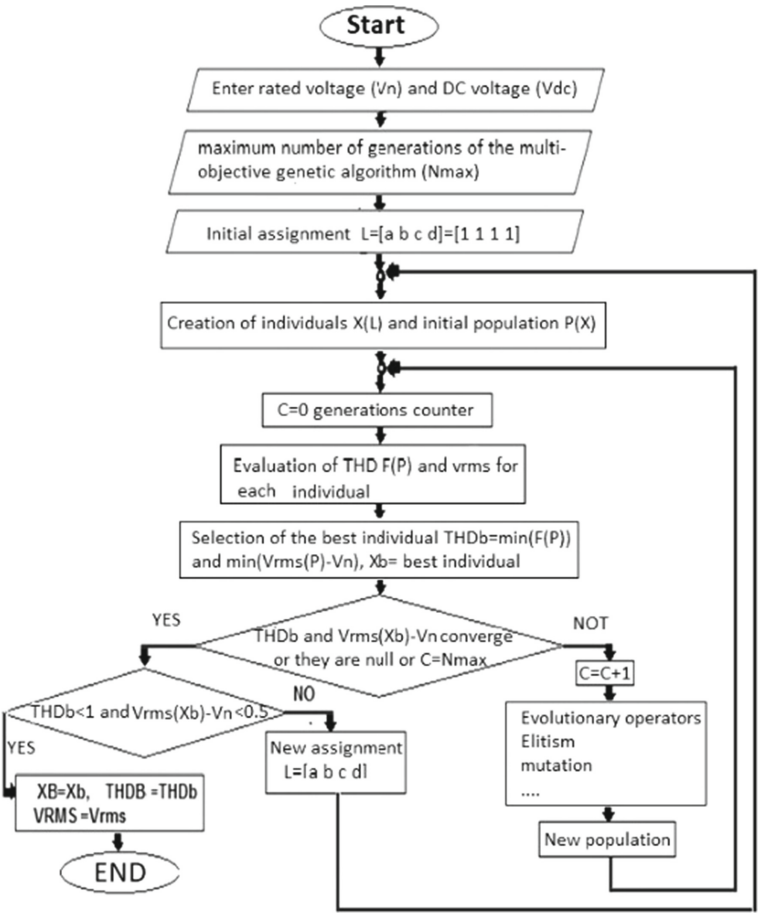

Fig. 2. Multi-objective genetic algorithm for optimization of V vs f.

If this stage ends, the algorithm verifies that the THD is less than 0.1% and that the value of the RMS line voltage approaches the desired value with a ± 0.5 V margin, if this does not happen the algorithm assigns a new vector L = [a b c d] and iterate the evolutionary part again, until the conditions are met. When the conditions are achieved, the algorithm stores the vector of switching angles, the RMS voltage and the THD value in a matrix, for the given frequency.

With the help of Matlab® and the *gamultiobj* command, the algorithms corresponding to the mathematical model of the fitness functions (THD and VRMS equations) and their respective optimization using multiobjective genetic algorithms were programmed. The population size for the algorithm is taken from 20 individuals, each individual (X) made up of the total of switching angles in the first quarter wave of the phase voltage, accompanied by the vector L, which indicates the program in charge of evaluate the fitness function the angles correspond to each step. The rated value of the voltage was assigned in 220 V, the rated frequency 60 Hz, the rated voltage of the DC block of 45 V.

5 Results of the Optimization Algorithm

The vector L was determined by the algorithm as L = [5 7 9 27]. It means that the best individual is composed of 48 switching angles in the first quarter of the waveform. The phase voltage waveform modulation of this individual is shown in Fig. 4. This individual presents an RMS value of 219.99 V and a THD of 0.00006% theoretical line, in phase the THD is 0.000067% and the value RMS voltage is 127.011 V. The harmonic spectrum of this waveform with the voltage amplitude found by the algorithm is shown in Fig. 3. The phase voltage spectrum shows that there is no significant contribution of harmonics. It is seen at first glance as a zero harmonic content of the first 50 harmonics. The three-phase voltage system is generated by three phases with the same waveform of Fig. 4, but with a phase shift of 120 electrical degrees, as shown in Fig. 5 and additionally the harmonic spectrum.

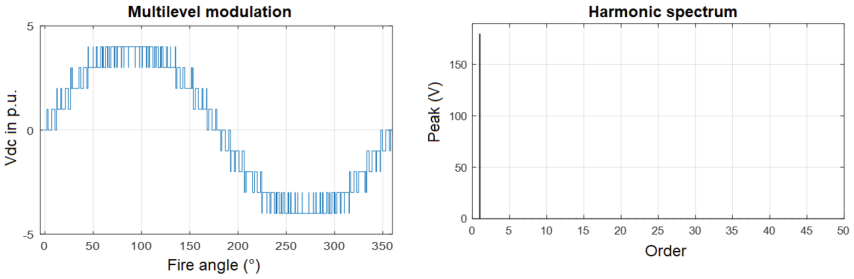

Fig. 3. PWM voltage waveform and spectrum of phase modulation.

For the population with individuals $L = [5\ 7\ 9\ 27]$, the evolution of the THD value is shown in Fig. 4. Where it is clearly observed that the THD value is null.

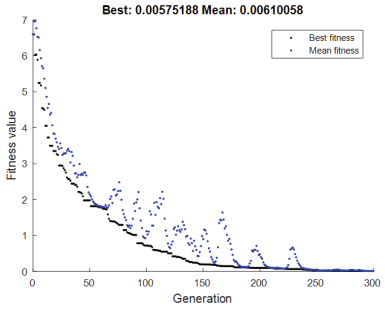

Fig. 4. Algorithm evolution for the population with individuals $\mathbf{L} = [5\ 7\ 9\ 27]$.

It takes the algorithm 300 generations to find the solution to the main function and the constraint, and it ends due to convergence as the maximum number of generations is not reached. As the variation is less than 0.00001 between two generations, the evolution is finished and when the convergence conditions are met, the general algorithm ends.

It is notable that additional steps and pulses appear in the line voltage, due to the subtraction that takes place between the phases. The phase modulation has 9 steps, while the line modulation has 17 steps, this makes the waveform closer to a sine waveform and therefore the harmonic content decreases substantially. The harmonic spectrum of the line voltages is shown in the same figure. In this spectrum it is clearly seen that the harmonic content is zero as in the phase voltages. The THD value of this calculated modulation is 0.0006% and the RMS value of the line voltage is 219.99 V.

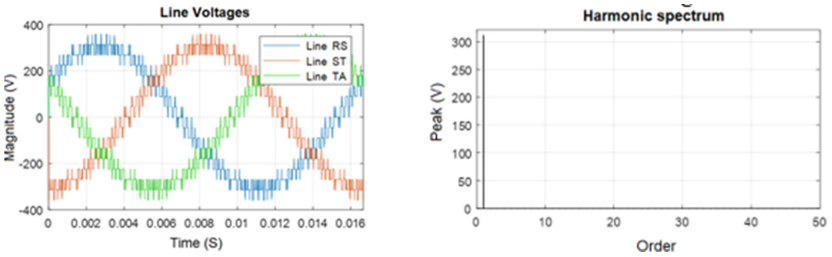

Fig. 5. PWM line voltage and spectrum of the positive sequence three-phase system.

6 Prototype Implementation

The power inverter and the DC/DC converter were implemented in a prototype of 2400 VA at rated frequency of 60 Hz. The rated input voltage is 48 V, its maximum value at the input can reach up to 70 V. The rated voltage of the line voltages is 220 V and the phase voltages 127 V. The control of the DC/DC converter and the power inverter was developed on a Virtex 5 FPGA.

6.1 Control Algorithm

To implement a voltage control that allows to preserve an optimal power quality, regardless of what happens in the load or in the accumulator block. Therefore, the DC/DC converter is connected to the power supply through the accumulator block and the output of the DC/DC converter to the multilevel power inverter. Using this as the internal connection of the prototype. The aim with this topology is that the DC/DC converter increases or decreases the value of the input voltage of the inverter. It is intended that the line voltage at the inverter output always remains the same regardless of the current required by the load, the voltage value given by the batteries or the regulation present in the prototype. The measured variable is the inverter output line voltage, this voltage is obtained with the measurement of the designed voltage sensor, which converts the RMS value of the voltage into a DC value.

The output signal of the voltage sensor is obtained using the NI USB 6009 DAQ. It is connected to a computer in which the control algorithm was developed in Labview. This algorithm has its respective graphical user interface in which the voltage set-point is assigned, in this case to a RMS voltage is 220 V. The Labview algorithm commands are communicated through the serial port to the Virtex 5 FPGA, which directly controls

the DC/DC converter by increasing or decreasing the output voltage. As required by the control (Labview) of the multilevel converter, always generating the same waveform. In short, the inverter control is static, always giving the same signals so that the inverter always generates the same waveform. In this way the control loop is established. Figure 6 shows the block diagram of the different elements involved in the control of the prototype.

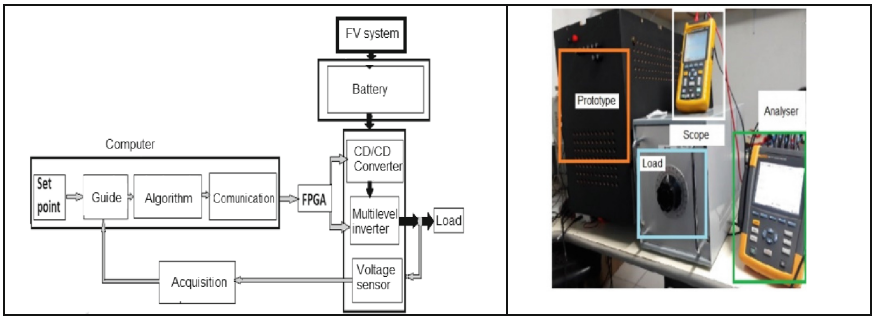

Fig. 6. Implementation of the converter a) Algorithm b) Experimental setup.

As previously mentioned, the voltage set-point was assigned to 220 V. This is adjusted by means of a graphical interface programmed in Labview®, which allows to visualize the output voltages and the reference voltage, as well as the controller actions. The Labview algorithm has the required scaling for the sensor and the output variable, as does the PID controller in the control loop.

7 Experimental Results

To validate the operation of the prototype, the converter is powered by the accumulator block of the photovoltaic system. Additionally, through the power converter, power is supplied to a three-phase load represented by a variable rheostat in order to be able to vary the operating points. The experimental setup is shown in Fig. 5b, where the elements of the system were labeled.

During the tests, the voltages and currents feeding the load were measured and the quality of the power delivered by the power converter was evaluated. In this way the voltage of the accumulator block and the current flowing from it to the prototype are measured. To evaluate the power quality of the converter, the Fluke 434 network analyzer was used, a device that has the ability to evaluate all power quality phenomena except for transient phenomena. Similarly, the NI USB 6211 acquisition card was used to capture the measurement of the line voltage from the sensor and the signal from the Fluke DP 120 voltage probe used to capture the voltage of the accumulator block and thus be able to establish the voltage profiles.

In the test the load was varied and the accumulator block was allowed to discharge deeply. With the intention of verifying the operation of the control loop and that the power quality of the output voltages and currents remain within the limits established by standards such as IEEE 1159 [19] and IEEE 519 [18]. The waveforms of the phase

voltages and their harmonic spectrum were captured by the network analyzer and are shown in Fig. 7.

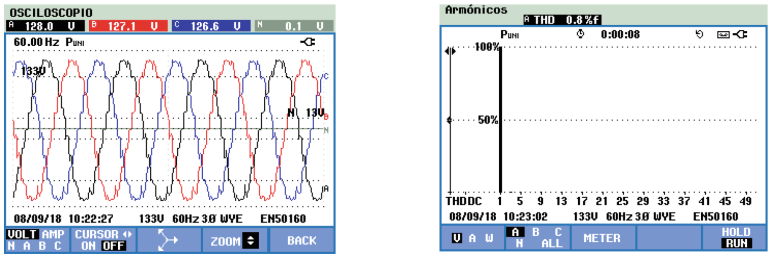

Fig. 7. Waveform and harmonic spectrum of phase voltages.

As can be seen in the figure, the three waveforms are the same. However there are small differences in the RMS value due to the construction of the transformers. The unbalance percentage of the voltages reaches just 0.6%, being well below 2% allowed in low voltage. The spectrum of the phase voltages shows that there is no significant presence of harmonics of any order and the total harmonic content is only 0.8%.

The waveforms of the line voltages are shown in Fig. 8.

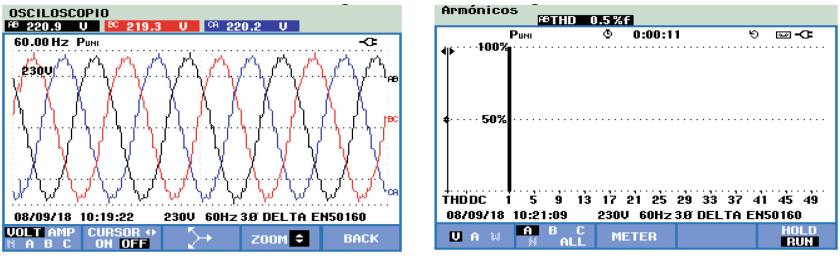

Fig. 8. Waveform and harmonic spectrum of line voltages

As can be seen in the figure, the three waves are equal in shape, presenting an almost sine waveform. However, they present different RMS values due to the differences between each of the phases due to the magnetic coupling between phases and the manual construction of the transformers. The harmonic spectrum captured by the analyzer for the line voltages is shown in Fig. 10. This spectrum, which evaluates the first 50 harmonics, shows that there is no significant presence of harmonics of any order and that the total harmonic content is less than 0.5%. This is characteristic of a pure sine waveform that guarantees an excellent quality of the power delivered by the power converter, in terms of harmonic content, it can be considered optimal.

Regarding the converter output current, the waveforms and spectrum are shown in Fig. 9.

As the converter is connected in a star connection, the line currents are equal to the phase currents, as can be seen, these are presented in an almost sinusoidal shape, with small variations. All three waveforms are identical in shape, presenting a nearly sinusoidal waveform. The harmonic spectrum shows that there is no significant presence of harmonics of any order and the total harmonic content is 1.2%, which is quite low.

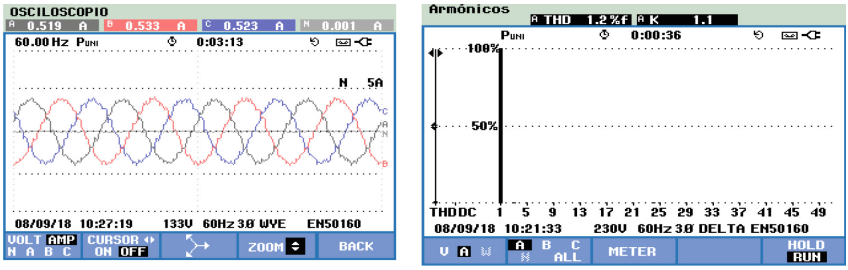

Fig. 9. Waveform and harmonic spectrum of line currents

The system of voltages are perfectly balanced in phases. Because the phase angle shows an exact 120° phase phase shift. To show the behavior of the voltage at the output of the converter, Fig. 10a shows the variation with respect to time, this figure is called the voltage profile.

The power converter line RMS volatility profile shows that the output behaves in a constant manner. Presenting a small ripple that can be neglected because the voltage is always in the range of 90% and 110% of the rated voltage that is established as the normal operating range in power quality. This means that, since there are no voltage fluctuations, the power quality phenomena associated with the RMS value are eliminated, these phenomena are sag, swell, overvoltage, undervoltage, interruptions and flicker.

The ripple presented at the output voltage does not exceed the magnitude of one volt. This ripple does not generate flickers since it is too low to be noticed by a lamp, and as it is always in the range of 90% to 10% of the rated voltage, it can be said that it is free from power quality phenomena.

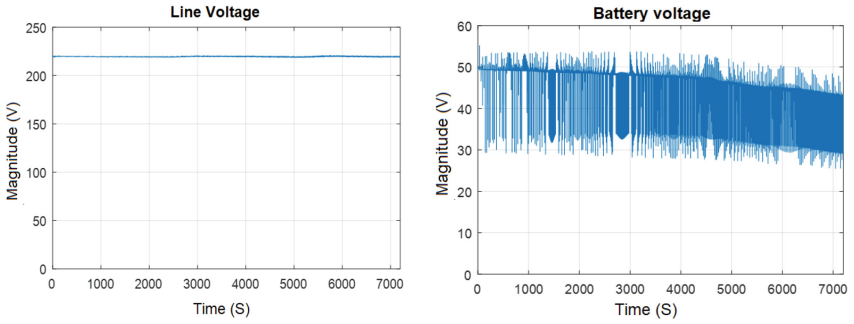

Fig. 10. a) Line voltage profile at the inverter output b) Voltage profile at the inverter input.

The voltage profile of the accumulator block during the test is shown in Fig. 10b. This shows how the input voltage to the power converter varies.

The voltage profile of the accumulator block shows that there are strong variations at the input, due to the current draw required by the prototype. The average voltage decreases as time passes, the initial value of the accumulator block is 52 V, at the end of the test the accumulator block voltage is 43 V. Despite the variations in the accumulator block and the voltage regulation that occurs over time, the voltage at the converter output remains constant over time. This means that the proposed control loop works in an adequate way, managing to mitigate the possible swell, sag, undervoltage and overvoltage that may occur due to the voltage variation of the accumulator block.

8 Conclusions

The developed prototype optimizes the power quality of photovoltaic systems by eliminating the possibility of phenomena such as sag, swell, undervoltage, overvoltage, harmonic distortion, flicker, frequency deviations, inter-harmonic, subharmonic distortion, DC component and notches. The only phenomena that the team does not cover are transitory phenomena and unbalances.

The harmonic contents found in the experimentation are very good both in the phase voltages and in the line voltages, in the same way the current also presents optimized contents, however, they do not become the same as those calculated theoretically, this is due to the presence of transformers that inject disturbances between phases and does not reproduce the pulses accurately. It is worth noting that the harmonic contents found present very low magnitudes, reaching values of 0.6%.

When implementing three-phase transformers for the H-bridge stages, the phases are coupled to each other, which generates disturbances between phases, however, this arrangement has an advantage and that is that the lack of a phase does not prevent the converter from continuing to operate. that it would work like an open star generating the third phase as a phantom phase.

In the validation, the power converter was presented at different operating points that demonstrated that the quality of the power at the output of the prototype was excellent. However, it is suggested to run a posteriori tests on the influence of the power factor on variables such as electric current.

References

1. Deshpande, S., Bhasme, N.R.: A review of topologies of inverter for grid connected PV systems. In: 2017 Innovations in Power and Advanced Computing Technologies (i-PACT), pp. 1–6 (2017)
2. Barater, D., Lorenzani, E., Concari, C., Franceschini, G., Buticchi, G.: Recent advances in single-phase transformerless photovoltaic inverters. IET Renew. Power Gener. **10**(2), 260–273 (2016)
3. Gaikwad, V., Mutha, S., Mundhe, R., Sapar, O., Chinchole, T.: Survey of PWM techniques for solar inverter. In: 2016 International Conference on Global Trends in Signal Processing, Information Computing and Communication (ICGTSPICC), pp. 501–504 (2016)

4. Saleh, S.A., Rahman, M.A.: Modeling of power inverters. In: An Introduction to Wavelet Modulated Inverters, p. 1. IEEE (2011)
5. Saleh, S.A., Rahman, M.A.: Introduction to power inverters. In: An Introduction to Wavelet Modulated Inverters, p. 1. IEEE (2011)
6. Ruderman, A.: About voltage total harmonic distortion for single- and three-phase multilevel inverters. IEEE Trans. Ind. Electron. **62**(3), 1548–1551 (2015)
7. Abu-Rub, H., Malinowski, M., Al-Haddad, K.: Multilevel converter/inverter topologies and applications. In: Power Electronics for Renewable Energy Systems, Transportation and Industrial Applications, p. 1. IEEE (2014)
8. Wu, B., Narimani, M.: Other multilevel voltage source inverters. In: High-Power Converters and AC Drives, p. 1. IEEE (2017)
9. Nabae, A., Takahashi, I., Akagi, H.: A new neutral-point-clamped PWM inverter. IEEE Trans. Indus. Appl. **IA-17**(5), 518–523 (1981). https://doi.org/10.1109/TIA.1981.4503992
10. Koshti, A.K., Rao, M.N.: A brief review on multilevel inverter topologies. In: 2017 International Conference on Data Management, Analytics and Innovation (ICDMAI), pp. 187–193 (2017)
11. Ghosh, G., Sarkar, S., Mukherjee, S., Pal, T., Sen, S.: A comparative study of different multilevel inverters. In: 2017 1st International Conference on Electronics, Materials Engineering and Nano-Technology (IEMENTech), pp. 1–6 (2017)
12. Roberge, V., Tarbouchi, M., Okou, F.: Strategies to accelerate harmonic minimization in multilevel inverters using a parallel genetic algorithm on graphical processing unit. IEEE Trans. Power Electron. **29**(10), 5087–5090 (2014)
13. Jacob, T., Suresh, L.P.: A review paper on the elimination of harmonics in multilevel inverters using bioinspired algorithms. In: 2016 International Conference on Circuit, Power and Computing Technologies (ICCPCT), pp. 1–8 (2016)
14. Srndovic, M., Zhetessov, A., Alizadeh, T., Familiant, Y.L., Grandi, G., Ruderman, A.: Simultaneous selective harmonic elimination and THD minimization for a single-phase multilevel inverter with staircase modulation. IEEE Trans. Ind. Appl. **54**(2), 1532–1541 (2018)
15. Anurag, A., Deshmukh, N., Maguluri, A., Anand, S.: Integrated DC–DC converter based grid-connected transformerless photovoltaic inverter with extended input voltage range. IEEE Trans. Power Electron. **33**(10), 8322–8330 (2018)
16. Fernandez, L.D.P., Rodriguez, J.L.D., Carvajal, M.A.J.: Three-phase multilevel inverter with selective harmonic elimination. In: 2015 Workshop on Engineering Applications - International Congress on Engineering (WEA), pp. 1–6 (2015)
17. Rodriguez, J.L.D., Fernandez, L.D.P., Garcia, A.P.: Harmonic distortion optimization of multilevel PWM inverter using genetic algorithms. In: 2014 IEEE 5th Colombian Workshop on Circuits and Systems (CWCAS), pp. 1–6 (2014)
18. IEEE Recommended Practice and Requirements for Harmonic Control in Electric Power Systems. IEEE Std 519–2014 (Revision of IEEE Std 519–1992). pp. 1–29 (2014)
19. IEEE Recommended Practice for Monitoring Electric Power Quality. IEEE Std 1159–2009 (Revision of IEEE Std 1159–1995). pp. c1–81 (2009)